

Comparative analysis of electronic structure and optical properties of crystalline and amorphous silicon nitride

S. Zh. Karazhanov,^{1,2} P. Kroll,^{3†} A. Holt¹, A. Bentzen,⁴ and A. Ulyashin^{1††}

¹Institute for Energy Technology, P.O.Box 40, NO-2027 Kjeller, Norway

²Department of Chemistry, University of Oslo, PO Box 1033 Blindern, N-0315 Oslo, Norway

³Institut für Anorganische Chemie, Rheinisch-Westfälische Technische Hochschule (RWTH),
Aachen, Landoltweg 1, 52056 Aachen, Germany

⁴REC Solar AS, P.O. Box 594, NO-1302 Sandvika, Norway

Abstract

We present a study of the electronic structure and optical properties of Si_3N_4 and $\text{Si}_2\text{N}_3\text{H}$ in crystalline and amorphous phases by first-principles calculations. We find that besides structural disorder those matrix atoms with dangling and floating bonds contribute to energy levels close to the Fermi-level. From a comparative analysis of calculated optical spectra we conjure that the difference in optical properties between crystalline and amorphous silicon nitride – either hydrogenated or un-hydrogenated – is only small. It is present mainly in the energy range close to the fundamental band gap. At larger energies the difference is negligible. It is found that the structuring disorder in silicon nitrides investigated does not affect essentially the electronic structure and optical properties of these materials. It is concluded that such amorphous silicon

nitrides can be used instead of their crystalline counterparts for various applications in which optical properties of such materials are important.

Keywords: silicon nitride, band gap, electrical properties, optical properties.

PACS: 31.15.Ar; 61.43.-j; 61.43.Bn; 61.43.Dq; 78.20.-e; 71.15.Pd; 71.20.-b

[†]Present address: Department of Chemistry and Biochemistry, The University of Texas at Arlington, Arlington, Texas 76019-0065, USA

^{††}SINTEF, Materials and Chemistry, P.O. Box 124 Blindern, NO-0314 Oslo, Norway

1. Introduction

Silicon nitride has found a wide range of applications in different fields as structural (automobile engines parts, cutting tools, nuclear reactors) and electronic material (dielectric, Si based integrated circuits, optoelectronics).¹ In semiconductor electronics $\text{SiN}_x\text{:H}$ prepared by plasma-enhanced chemical vapour deposition is widely used. Interest to $\text{SiN}_x\text{:H}$ is because it is mechanically strong, provide excellent barrier against mobile ions and corrosion, it can contain large amount of H atoms, needed for passivation of bulk and surface defects, large fundamental band gap (>3 eV), and low extinction coefficient.^{2, 3} To improve applicability of *am*- $\text{SiN}_x\text{:H}$ in electronics, however, a deeper understanding of its electronic structure and optical properties is needed both theoretically and experimentally. The scientific literature presents several theoretical and experimental studies of properties of crystalline (*cr*) and amorphous (*am*) phases of pure and defective, hydrogenated and non-hydrogenated silicon nitride materials (see Refs.^{1, 4-10}). Core-level and valence band photoemission studies addressed the origin of the conduction band (CB) minimum and valence band (VB) maximum as well as the influence of H on these parts of the electronic structure⁴. Accordingly, N $2p$ states contribute most to the VB maximum of SiN_x for $x > 1.1$. However, if $x < 1.1$, then the VB maximum is dominated by Si $3p$ electrons. Similarly, the CB minimum is determined by Si $3s$ electrons for $x < 1.25$, while hybridized Si $3s$, $3p$, and N $2p$ states dominate, if $x > 1.25$. Soft-x-ray emission studies indicate that the spectra of the crystalline α - and β -phases of Si_3N_4 are similar to each other.¹¹ First-principles electronic structure calculations¹⁰ are in agreement with these result.

Focusing on amorphous hydrogenated silicon nitride, *am*- $\text{SiN}_x\text{:H}$, x-ray photoemission spectroscopy (XPS), electron-energy-loss spectroscopy, and optical absorption studies showed that the optical gap opens up once the ratio of Si-Si to N-H bonds falls below 0.10.⁹ The

incorporation of hydrogen also causes shift of the Fermi level in $\text{SiN}_x\text{:H}$ by 0.5-0.7 eV towards the conduction band (CB).⁴ Hydrogen related bonding states are located at 6.3 eV and 9.8 eV below the VB maximum.⁴ Current-voltage characteristics of charge transport through $\text{SiN}_x\text{:H}$ films suggest to obey small-polaron transport.¹²

Several experimental studies addressed optical properties of SiN_x films. Spectroscopic ellipsometry using conventional and synchrotron-radiation light sources has been used to measure the optical response of SiN_x prepared by different techniques in the energy range from 1.5-9.5 eV.¹³ A dual role of H in the fundamental band gap E_g has been noticed: it can cause an increase⁹ and reduction of E_g .¹³ A shift of the optical spectra towards lower energies with increasing the H concentration¹³ has been ascribed to H induced reduction of both band gaps. Soft x-ray studies showed drastic H-induced change in the density, network, and surface morphology of SiN_x .¹⁴

Theoretical studies within the framework of density functional theory (DFT) have been employed to study band structure, effective masses, density of states, charge density, chemical bonding, and optical properties of different polymorphs of *cr*- Si_3N_4 .¹ Amorphous silicon nitride structures (*am*- SiN_x and *am*- $\text{SiN}_x\text{:H}$) have also been studied. Model structures were generated by either molecular dynamics simulations or by a network forming approach^{7, 15-18}. While all modeling approaches battle with substantial amounts of structural defects in the disordered models, the network approach emerged as the most efficient tool to generate reliable structural models of amorphous SiN_x ,⁵ $\text{SiN}_x\text{:H}$,⁷ and $\text{Si}_2\text{N}_2\text{O}$ ¹⁵ with well-defined bond topology.

Results of the modeling studies indicate that stoichiometric *am*- Si_3N_4 exhibits substantial internal stresses, responsible for the development of topological defects such as dangling (three-fold coordinated Si and two-fold coordinated N) and floating (five-fold coordinated Si and four-

fold coordinated N) bonds. Introducing H and O atoms into the structure, thus, lowering the average connectivity of the network, then reduces considerably the internal strain in amorphous silicon nitride. Their impact on the electronic structure and optical properties is also drastic. Hydrogenation of a defect-rich disordered structure obviously reduces the concentration of band gap states through termination of dangling bonds.⁸ Even small amount of H effects considerably the electronic structure and optical properties of silicon nitride.^{5, 7} While these initial considerations were encouraging, the science around silicon nitride lacks a systematic analysis of influence of structural disorder and impact of hydrogen on the optical properties of silicon nitride.

The aim of this work, therefore, is to perform a comparative analysis of the electronic structure and the optical properties of *cr*-Si₃N₄, *am*-Si₃N₄, *cr*-Si₂N₃H, and *am*-Si₂N₃H. To anticipate our results, we found that levels close to the fundamental edge are most impacted by structure and chemistry of the amorphous phase. Consequently, control over the latter allows to adjust and finetune the former.

2. Methods

2.1 Computational details

The *cr*- and *am*- modifications of Si₃N₄ and Si₂N₃H are schematically presented in Fig. 1. Structural data of *cr*-Si₃N₄ (α - and β -Si₃N₄) and *cr*-Si₂N₃H was taken from Refs. ¹⁹ and ²⁰, respectively (Table I). Models of stoichiometric *am*-Si₃N₄ and of hydrogenated *am*-SiN_x:H were generated using the network approach together with subsequent *ab initio* molecular dynamics simulations.⁵⁻⁷ The models of *am*-Si₃N₄ and *am*-Si₂N₃H consist of 112 and 144 atoms, respectively.

The band-structure calculations have been performed using the Vienna *ab initio* simulation package (VASP),^{21, 22} which calculates the Kohn—Sham eigenvalues in the framework of the DFT within the local density approximation (LDA). The exchange and correlation energy of electrons is described through the Perdew-Zunger parametrization²³ of the quantum Monte Carlo results of Ceperley-Alder.²⁴ We use the projector-augmented wave (PAW) method.^{25, 26} Atomic cores are described by pseudopotentials as implemented in the VASP package. The application of the pseudopotentials allows us to construct orthonormalized all-electron-like wave functions for the Si-4s and -4p, N-2s and -2p, and H-1s valence electrons. Spin-orbit coupling was not included in the present calculations.

Imaginary part of the dielectric function $\varepsilon_2(\omega)$ was calculated by the DFT within LDA approximation.^{27, 28}

$$\varepsilon_2^{ij}(\omega) = \frac{Ve^2}{2\pi\hbar m^2 \omega^2} \int d^3k \sum_{mn} \langle kn | p_i | kn' \rangle \langle kn' | p_j | kn \rangle \times f_{kn} (1 - f_{kn'}) \delta(f_{kn'} - f_{kn} - \hbar\omega). \quad (1)$$

Here $(p_x, p_y, p_z) = p$ is the momentum operator, f_{kn} is the Fermi distribution, and $|kn\rangle$ is the crystal wave function, corresponding to energy ε_{kn} with momentum k . $V/8\pi^3$ is the normalization constant of the integral over reciprocal space. More computational details can be found in Refs.^{27, 28}. The trigonal and hexagonal structures of α - and β -Si₃N₄ are optically anisotropic, thus two components of the dielectric function corresponding to the electric field parallel ($E||c$) and perpendicular ($E\perp c$) to the crystallographic c axis have been considered. For orthorhombic Si₂N₃H three components of $\varepsilon_2(\omega)$ have been considered. Six components of optical spectra have been calculated for the amorphous structures. In the paper we have presented the results for the direction $E\perp c$. To facilitate the comparison with experimental data^{25,26}, we applied a broadening using a Lorentzian function with a FWHM of 0.002 eV.

The real part of the dielectric function $\varepsilon_1(\omega)$ is then calculated using the Kramers-Kronig transformation. The two dielectric functions were then used to calculate other optical properties. In this paper, we presented the absorption coefficient $\alpha(\omega)$, the reflectivity $R(\omega)$, the refractive index $n(\omega)$, and the extinction coefficient $k_e(\omega)$ calculated using the following expressions:

$$R(\omega) = \left| \frac{\sqrt{\varepsilon(\omega)} - 1}{\sqrt{\varepsilon(\omega)} + 1} \right|^2, \quad (2)$$

$$\alpha(\omega) = \sqrt{2}\omega \sqrt{\sqrt{\varepsilon_1^2(\omega) + \varepsilon_2^2(\omega)} - \varepsilon_1(\omega)}, \quad (3)$$

$$n(\omega) = \sqrt{\frac{\sqrt{\varepsilon_1^2(\omega) + \varepsilon_2^2(\omega)} + \varepsilon_1(\omega)}{2}}, \quad (4)$$

$$k_e(\omega) = \sqrt{\frac{\sqrt{\varepsilon_1^2(\omega) + \varepsilon_2^2(\omega)} - \varepsilon_1(\omega)}{2}}. \quad (5)$$

Here $\varepsilon(\omega) = \varepsilon_1(\omega) + i\varepsilon_2(\omega)$ is the complex dielectric function. The optical spectra are calculated by DFT within LDA approximations for the energy range 0-14 eV.

3. Results and discussion

3.1 Bond length distribution

In Figure 2 we show the Si-N bond length distribution for the crystalline compounds α - and β -Si₃N₄, and *cr*-Si₂N₃H as well as for the amorphous structures of *am*-Si₃N₄ and *am*-Si₂N₃H. The crystalline structures have well-defined Si-N bond lengths of about 1.73 Å, while the amorphous models show a much broader distribution of Si-N bond lengths, including some pretty long interaction distances up to 2.2 Å. Previous computational studies, however, indicated that a

significant medium-range order up to the neighbour shell persists in the amorphous state of Si_3N_4 and $\text{Si}_2\text{N}_3\text{H}$.^{7, 18}

We analyzed the bond coordination in detail for all the silicon nitride structures for distances lengths $\leq 2.0 \text{ \AA}$ (Table II). α - and β - Si_3N_4 exhibit Si four-fold coordinated by N and N three-fold coordinated by Si.^{1, 9} The model structure of *am*- Si_3N_4 comprises one single Si atom in three-fold coordination to N, while three Si have five bonds to adjacent N atoms. Two N possess two coordinated bond, four N possess four coordinated bonds. In *cr*- $\text{Si}_2\text{N}_3\text{H}$ ($=\text{Si}_2\text{N}_2(\text{NH})$) Si atoms are also four-fold coordinated by N. Two types of N exist, one N three-fold coordinated by Si the other bonded to two Si and one H. The model structure of *am*- $\text{Si}_2\text{N}_3\text{H}$ comprises all Si four-fold coordinated by N, and in so far resembles the crystalline structure. The detailed coordination of N atoms, however, is more complicated. The majority of N atoms are three-fold coordinated to Si. While this resembles the crystal structure as well, some topological defects appear. For both amorphous model structures we observe that topological defects develop primarily at N atoms. Moreover, optimized models of *am*- Si_3N_4 tend to have an average coordination number for Si and N slightly larger than the crystal structure values of 4 and 3, respectively.²⁹ The above results confirm validity of amorphous nature of *am*- Si_3N_4 and *am*- $\text{Si}_2\text{N}_3\text{H}$.

3.2 Density of states

Figure 3 displays the total densities of states (DOS) of α - and β - Si_3N_4 , *am*- Si_3N_4 , *cr*- $\text{Si}_2\text{N}_3\text{H}$, and *am*- $\text{Si}_2\text{N}_3\text{H}$ in the energy range from -3 to +6 eV. The fundamental band gaps E_g have been determined as the difference of energies corresponding to the VB and CB edges. The magnitude of E_g is equal to 4.6 eV for α - Si_3N_4 , 4.2 eV for β - Si_3N_4 , ~3.5 eV for *am*- Si_3N_4 , 5.0

eV for *cr*-Si₂N₃H, and ~3.4 eV for *am*-Si₂N₃H. Total DOS for *am*-Si₃N₄ and *am*-Si₂N₃H possesses tails in the band gap formed due to lattice disorder and under/over -coordinated structural defects. The calculated band gaps agree well with those of Refs. ^{1, 5}. However, those for α - and β -Si₃N₄ are smaller than 4.7-4.9 eV determined¹¹ from analysis of the soft x-ray emission spectra for these two polymorphs. The fundamental band gap 5.4 eV of *am*-Si₃N₄ determined³⁰ from the energy loss spectra of N 1s photoelectrons is larger than the calculated 3.5 eV. There are no experimental data for both *cr*- and *am*-Si₂N₃H. The experimental results for the band gap of SiN_x:H is available for $x \approx 1.3$, which is in the range 4.5-5.0 eV.⁸ As expected the calculated band gaps are underestimated than the experimentally measured ones due to the well known deficiency of DFT. The band gap for *cr*-Si₂N₃H is much larger than that of α - and β -Si₃N₄. This result is consistent with experimental and theoretical results regarding H induced widening the band gap.⁹

Insight into the bonding interaction between constituents and the origin of CB and VB electronic energy levels can be obtained from the analysis of the site and orbital projected (PDOS) presented in Fig. 4. The lowest bands located in the energy range from -20 eV to -14 eV are mainly contributed by N 2s electrons with noticeable Si 3p and 3s electrons. The upper part of the VBs' located in the energy range from -9 to 0 eV is basically contributed from Si 3p and N 2p states. Bottommost CB of α - and β -Si₃N₄, *am*-Si₃N₄, as well as *cr*- and *am*-Si₂N₃H is basically contributed from Si 3p and 3s and N 2s and 2p electrons. These results are consistent with previous theoretical¹ and experimental^{4, 31} results.

3.3 Optical properties

The calculated optical spectra for the α - and β -Si₃N₄, *am*-Si₃N₄, and *cr*- *am*-Si₂N₃H are presented in Fig. 5. The imaginary part of the optical dielectric response function, absorption

coefficient, and reflectivity spectra have been analyzed. Since crystal structures of the Si_3N_4 phases are hexagonal, the optical spectra of the electric field components perpendicular ($E \perp c$) and parallel ($E \parallel c$) to the c -axes should both be analyzed. Our analysis showed that optical spectra of Si_3N_4 between these two directions are almost the same in the energy ranges from 0-8 eV and 11.5-20 eV. So, optical spectra for the direction $E \perp c$ have been analysed for all the structural modifications of silicon nitride considered in the present paper.

As noted above, the fundamental band gap has been underestimated because of the deficiency of the DFT. Consequently, the calculated optical spectra in Fig. 5 are shifted toward lower energies than the really existing ones. Since the SiN_x and $\text{SiN}_x\text{:H}$ do not contain d electrons included into the valence complex, the band gap underestimation and shift of the optical spectra are not as severe as, say, in ZnO. Often the rigid shift technique is applied to fix partially the band gap problem. The way of correcting the band gap has not been applied here. The calculated optical spectra have been compared with the experimental results for SiN_x prepared by spray pyrolysis³² and chemical vapour deposition.¹³

Analysis of Fig. 5 shows that absorption of $am\text{-Si}_3\text{N}_4$ and $\text{-Si}_2\text{N}_3\text{H}$ starts at ~ 4.8 eV, whereas that of $cr\text{-Si}_3\text{N}_4$ and $\text{-Si}_2\text{N}_3\text{H}$ starts from ~ 5.0 eV. The difference in the absorption edge energies shows that band tails of $am\text{-Si}_3\text{N}_4$ plays important role in optical transitions. However, both $am\text{-}$ and $cr\text{-Si}_3\text{N}_4$ and $\text{Si}_2\text{N}_3\text{H}$ are transparent in the energy range of photons 0.0-4.8 eV. Furthermore, the absorption coefficient and reflectivity is lower than 10^5 cm^{-1} and 0.25, respectively.

The shift of the fundamental absorption edge of $am\text{-Si}_3\text{N}_4$ and $\text{-Si}_2\text{N}_3\text{H}$ toward lower energies compared to their crystalline counterparts is well-known to be due to absorption by the tail states located right up the topmost VB and below the bottommost CB of $cr\text{-Si}_3\text{N}_4$. At lower

energies 3-7.5~eV the absorption coefficient, reflectivity, refractive index, and the extinction coefficient of *am*-Si₃N₄ and -Si₂N₃H are larger than those of their crystalline counterparts. However, at higher energies in the range 7.5-20~eV the difference is negligible. Since, *am*-Si₃N₄ and -Si₂N₃H can more easily be formed than their crystalline counterparts, they can be used instead of the crystalline one.

Analysis of Fig. 5 shows that the optical spectra of both *cr*- and *am*-Si₃N₄ are shifted toward lower energies compared to those of *cr*- and *am*-Si₂N₃H. This result is consistent with the experimentally established result regarding the H induced widening of the fundamental band gap.⁹ Although the band gap calculated by DFT has been underestimated and the optical spectra has been shifted to lower energies, they are in good agreement with those for SiN_x prepared by SP and CVD techniques (Fig. 5). The reason of the deviation can be related to overestimation of the momentum matrix elements, neglect of the Coulomb interaction between free electrons and holes (excitons), local-field and finite lifetime effects. Furthermore, in the calculations of the imaginary part of the dielectric response function only direct optical transitions from occupied to unoccupied states have been considered. For the optical calculations, many more **k** points are needed in order to obtain convergence than in the ground-state calculation. Due to memory restrictions of the supercomputers in the present work number of **k** points in the irreducible Brillouin zone has slightly exceeded that used in the ground-state calculation for large supercells of *am*-Si₃N₄ and Si₂N₃H. Also, charge fluctuations and the experimental resolution smear out many fine features. These points might be the reasons of the above mentioned deviation between the theory and experiment.

Conclusion

Electronic structure and optical properties of *am*- and *cr*- Si_3N_4 and $\text{Si}_2\text{N}_3\text{H}$ are studied. Acceptor and donor type bands have been found in the band gap of *am*- Si_3N_4 and $\text{Si}_2\text{N}_3\text{H}$ formed by under/over-coordinated Si and N atoms and lattice disorder. No such bands are found in the fundamental bandgap of *cr*- Si_3N_4 and $\text{Si}_2\text{N}_3\text{H}$. From orbital and site projected density of states nature of the valence and conduction bands have been determined. It is shown that the topmost valence band mostly consists of Si and N *p* states. Conduction band minimum of both *am*- and *cr*- Si_3N_4 consist of well hybridized Si and N *s* and *p* orbitals. We found that optical properties of *am*- Si_3N_4 and $\text{Si}_2\text{N}_3\text{H}$ only slightly differ from those of crystalline counterparts. The difference is found in the energy range close to the fundamental band gap. At larger energies exceeding the fundamental band gap the difference is negligible. Both *am*- and *cr*- Si_3N_4 and $\text{Si}_2\text{N}_3\text{H}$ are found to be transparent in the visible spectra. Thus it can be concluded that the amorphous silicon nitrides, can be used instead of their crystalline counterparts for various applications such as antireflection coatings for solar cells etc., in which optical properties of such materials are important.

Acknowledgments

This work has been funded by REC, FUNMAT, and NANOMAT. Supercomputing support has been obtained through the Research Council of Norway.

References

- ¹ Y.-N. Xu and W. Y. Ching, *Phys. Rev. B* **51**, 17379 (1995).
- ² J. Yoo, S. Kumar Dhungel, and J. Yi, *Thin Solid Films* **515**, 7611 (2007).
- ³ A. G. Aberle, *Sol. Energy Mater. Sol. Cells* **65**, 239 (2001).
- ⁴ R. Kärcher, L. Ley, and R. L. Johnson, *Phys. Rev. B* **30**, 1896 LP (1984).
- ⁵ P. Kroll, *Mat. Res. Symp. Proc.* **715**, 479 (2002).
- ⁶ P. Kroll, *J. Non-Cryst. Solids* **293-295**, 238 (2001).
- ⁷ P. Kroll, in *Mat. Res. Symp. Proc.*, edited by S. Ashok, J. P. Chevallier, N. M. Johnson, B. L. Sopori and H. Okushi, 2002), Vol. 719, p. 283.
- ⁸ J. F. Justo, F. de Brito Mota, and A. Fazzio, *Phys. Rev. B* **65**, 073202 (2002).
- ⁹ M. M. Guraya, H. Ascolani, G. Zampieri, J. I. Cisneros, J. H. Dias da Silva, and M. P. Cantão, *Phys. Rev. B* **42**, 5677 (1990).
- ¹⁰ S.-Y. Ren and W. Y. Ching, *Phys. Rev. B* **23**, 5454 LP (1981).
- ¹¹ R. D. Carson and S. E. Schnatterly, *Phys. Rev. B* **33**, 2432 LP (1986).
- ¹² L. Martinmoreno, E. Martinez, J. A. Verges, and F. Yndurain, *Phys. Rev. B* **35**, 9683 (1987).
- ¹³ J. Petalas and S. Logothetidis, *Phys. Rev. B* **50**, 11801 LP (1994).
- ¹⁴ M. H. Modi, G. S. Lodha, P. Srivastava, A. K. Sinha, and R. V. Nandedkar, *Phys. Rev. B* **74**, 045326 (2006).
- ¹⁵ P. Kroll, *J. Non-Cryst. Solids* **351**, 1127 (2005).
- ¹⁶ P. Kroll, *J. Non-Cryst. Solids* **345-346**, 720 (2004).
- ¹⁷ P. Kroll, in *Mat. Res. Symp. Proc.*, 2002), Vol. 731, p. 249.

- ¹⁸ P. Kroll, in *Mat. Res. Symp. Proc.*, edited by J. D. Cohen, J. R. Abelson, H. Matsumura and J. Robertson, 2002), Vol. 715, p. 479.
- ¹⁹ in *Inorganic Crystal Structure Database* (Gmelin Institut, Karlsruhe, 2001).
- ²⁰ E. Horvath-Bordon, R. Riedel, P. F. McMillan, P. Kroll, G. Miehe, P. A. van Aken, A. Zerr, P. Hoppe, O. Shebanova, I. McLaren, S. Lauterbach, E. Kroke, and R. Boehler, *Angew. Chem. Int. Ed.* **46**, 1476 (2007).
- ²¹ G. Kresse and J. Hafner, *Phys. Rev. B* **47**, 558 (1993).
- ²² G. Kresse and J. Furthmüller, *Phys. Rev. B* **54**, 11169 (1996).
- ²³ J. P. Perdew and A. Zunger, *Phys. Rev. B* **23**, 5048 (1981).
- ²⁴ D. M. Ceperley and B. J. Alder, *Phys. Rev. Lett.* **45**, 566 (1980).
- ²⁵ P. E. Blochl, *Phys. Rev. B* **50**, 17953 (1994).
- ²⁶ G. Kresse and D. Joubert, *Phys. Rev. B* **59**, 1758 (1999).
- ²⁷ A. Delin, O. Eriksson, B. Johansson, S. Auluck, and J. M. Wills, *Phys. Rev. B* **60**, 14105 LP (1999).
- ²⁸ A. Delin, P. Ravindran, O. Eriksson, and J. Wills, *Int. J. Quantum Chem.* **69**, 349 (1998).
- ²⁹ P. Kroll, *J. Eur. Ceram. Soc.* **25**, 163 (2005).
- ³⁰ S. Miyazaki, M. Narasaki, A. Suyama, M. Yamaoka, and H. Murakami, *Appl. Surf. Sci.* **216**, 252 (2003).
- ³¹ V. A. Gritsenko, Y. N. Morokov, and Y. N. Novikov, *Appl. Surf. Sci.* **113-114**, 417 (1997).
- ³² H. R. Philipp, *J. Electrochem. Soc.* **120**, 295 (1973).

Table I. Primitive unit-cell dimensions, volumes, and structural parameters for *cr*- and *am*-Si₃N₄ and Si₂N₃H. Experimentally determined lattice parameters of Refs. ¹⁹ and ²⁰ (in brackets) have been used as input for *ab initio* studies of *cr*-Si₃N₄ and Si₂N₃H, respectively.

Compound	Space group	Unit cell (Å)	Atom	Site	<i>x</i>	<i>y</i>	<i>z</i>
α -Si ₃ N ₄	$P\bar{3}1$	<i>a</i> =7.808(7.752)	Si1	6 <i>c</i>	0.2535(0.2532)	0.1673(0.1672)	0.4508(0.4509)
		<i>c</i> =5.660(5.620)	Si2	6 <i>c</i>	0.0825(0.0822)	0.5122(0.5119)	0.6593(0.6580)
		<i>V</i> =298.81(292.45)	N1	6 <i>c</i>	0.6555(0.6550)	0.6096(0.6111)	0.4322(0.4297)
			N2	6 <i>c</i>	0.3143(0.3153)	0.3189(0.3197)	0.6968(0.7006)
			N3	2 <i>b</i>	0.3333(0.3333)	0.6667(0.6667)	0.6032(0.5999)
			N4	2 <i>a</i>	0.0000(0.0000)	0.0000(0.0000)	0.4513(0.4541)
β -Si ₃ N ₄	$P6_3$	<i>a</i> =7.572(7.602)	Si	6 <i>h</i>	0.1744(0.1773)	0.7682(0.7677)	0.2500(0.2500)
		<i>c</i> =2.896(2.907)	N1	2 <i>c</i>	0.3333(0.3333)	0.6667(0.6667)	0.2500(0.2500)
		<i>V</i> =143.79(145.46)	N2	6 <i>h</i>	0.3303(0.3333)	0.0304(0.0323)	0.2500(0.2500)
<i>am</i> -Si ₃ N ₄	<i>P</i> 1	<i>a</i> =11.878	Si	1 <i>a</i>			
		<i>b</i> =9.994	N	1 <i>a</i>			
		<i>c</i> =9.629, α =85.65,					
		β =88.55, γ =95.66					
		<i>V</i> =1133.62					
<i>cr</i> -Si ₂ N ₃ H	<i>Cmc</i> ₂ <i>1</i>	<i>a</i> =9.265(9.193)	Si	8 <i>b</i>	0.1744(0.1737)	0.1587(0.1560)	0.0179(0.0000)
		<i>b</i> = 5.456(5.410)	N1	8 <i>b</i>	0.2109(0.2130)	0.8750(0.8630)	0.1684(0.1500)
		<i>c</i> =4.857(4.819)	N2	4 <i>a</i>	0.5000(0.5000)	0.7581(0.7580)	0.0834(0.0700)
		<i>V</i> =245.49(239.65)	H	4 <i>a</i>	0.5000(0.5000)	0.0976(0.0968)	0.7185(0.8044)
<i>am</i> -Si ₂ N ₃ H	<i>P</i> 1	<i>a</i> =11.122	Si	1 <i>a</i>			
		<i>b</i> =10.072	N	1 <i>a</i>			
		<i>c</i> =12.178, α =89.97,					
		β =84.72, γ =97.26					
		<i>V</i> =1347.51					

Table II. Number of occurrences of bond coordinations in the unit cells of *cr*- and *am*- Si_3N_4 and $\text{Si}_2\text{N}_3\text{H}$ for atomic distances $< 2\text{\AA}$.

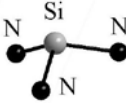
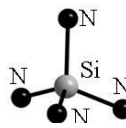
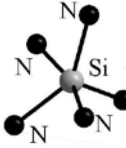
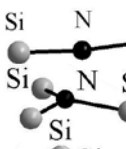
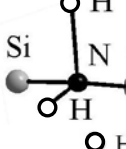
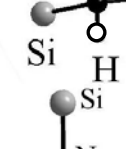
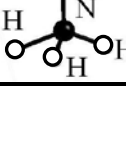
Bond coordination	$\alpha\text{-Si}_3\text{N}_4$	$\beta\text{-Si}_3\text{N}_4$	<i>am</i> - Si_3N_4	<i>cr</i> - $\text{Si}_2\text{N}_3\text{H}$	<i>am</i> - $\text{Si}_2\text{N}_3\text{H}$
			1		
	12	6	44	8	48
			3		
			2		
	16	8	59	8	47
			3		
					2
				4	16
					6
					1

Figure captions

Fig. 1. Schematic presentation of structures for (a) α - and (b) β - Si_3N_4 , (c) *am*- Si_3N_4 , (d) *cr*- $\text{Si}_2\text{N}_3\text{H}$, and (e) *am*- $\text{Si}_2\text{N}_3\text{H}$.

Fig. 2. Number of bonds per bond length for α - and β - Si_3N_4 , *am*- Si_3N_4 , *cr*- $\text{Si}_2\text{N}_3\text{H}$, and *am*- $\text{Si}_2\text{N}_3\text{H}$.

Fig. 3. Total DOS for α - Si_3N_4 , β - Si_3N_4 , *am*- Si_3N_4 , *cr*- $\text{Si}_2\text{N}_3\text{H}$, and *am*- $\text{Si}_2\text{N}_3\text{H}$. The Fermi level is set to zero.

Fig. 4. The orbital and site-projected DOS for α - and β - Si_3N_4 , *am*- Si_3N_4 , and *am*- $\text{Si}_2\text{N}_3\text{H}$. The Fermi level is set at zero of energy.

Fig. 5. Calculated optical spectra for α - and β - Si_3N_4 , *am*- Si_3N_4 , *cr*- $\text{Si}_2\text{N}_3\text{H}$, and *am*- $\text{Si}_2\text{N}_3\text{H}$ along with experimentally measured ones for *am*- SiN_x grown by spray pyrolysis³² and chemical vapour deposition.¹³ The absorption coefficients are given in [cm^{-1}] divided by 10^5 .